

SONNEBERG PLATE PHOTOMETRY FOR BOYAJIAN'S STAR IN TWO PASSBANDS

MICHAEL HIPPE,¹ PETER KROLL,² FRANK MATTHAI,² DANIEL ANGERHAUSEN,³ TAAVI TUVIKENE,⁴ KEIVAN G. STASSUN,⁵
ELENA ROSHCINA,⁶ TATYANA VASILEVA,⁶ IGOR IZMAILOV,⁶ AND MICHAEL B. LUND⁵

¹*Luiters Straße 21b, 47506 Neukirchen-Vluyn, Germany*

²*Sonneberg Observatory, Sternwartestr. 32, 96515 Sonneberg, Germany*

³*NASA Postdoctoral Program Fellow, NASA Goddard Space Flight Center, Exoplanets & Stellar Astrophysics Laboratory, Code 667, Greenbelt, MD 20771*

⁴*Tartu Observatory, Observatooriumi 1, 61602 Tõravere, Estonia*

⁵*Department of Physics and Astronomy, Vanderbilt University, Nashville, TN 37235, USA*

⁶*Main (Pulkovo) Astronomical Observatory of RAS, 196140, Russia, Saint-Petersburg, Pulkovskoye shosse 65*

ABSTRACT

The F3 main sequence star KIC 8462852 (Boyajian's Star) has raised interest because of its mysterious day-long brightness dips, and an unusual $\sim 3\%$ brightness decrease during the 4 years of the *Kepler* mission. Recently, a 0.164 mag ($\sim 14\%$) dimming between 1890 and 1990 was claimed, based on the analysis of photographic plates, although this has been challenged. To resolve this controversy, we have gathered an independent set of historic data from Sonneberg Observatory, Germany. From these historic plates, we could extract 861 magnitudes in blue light, and 397 magnitudes in red light. The data cover the years 1934 to 1995 and are very evenly sampled between 1956 and 1995. In both passbands, we find the star to be of constant brightness within 0.03 mag/century (2%). The previously claimed dimming is inconsistent with these data at the $\sim 5\sigma$ -level, however the recently reported modest dimming of $\sim 3\%$ in the Kepler data is not inconsistent with these data. We have also searched for periodicities and shorter trends in the data and find none that is significant within our limits of $\sim 5\%$ per 5-year bin.

1. INTRODUCTION

The *Kepler* Space Telescope’s exquisite photometry has allowed for the detection of more than a thousand exoplanets (Borucki et al. 2010). The data have also been used for a wide range of stellar studies (e.g., Huber et al. 2011; Hippke et al. 2015). One very peculiar object is Boyajian’s Star (KIC 8462852, TYC 3162-665-1). This is an F3 main-sequence star, which was observed by the NASA *Kepler* mission from April 2009 to May 2013. An analysis by Boyajian et al. (2016) shows inexplicable series of day-long brightness dips up to 20%. The behavior has been theorized to originate from a family of large comets (Bodman & Quillen 2016), or signs of a Dyson sphere (Wright et al. 2016). Subsequent analysis found no narrow-band radio signals (Harp et al. 2016) and no periodic pulsed optical signals (Schuetz et al. 2016; Abeysekara et al. 2016). The infrared flux is equally unremarkable (Lisse et al. 2015; Marengo et al. 2015; Thompson et al. 2016). Recently, the star has been claimed to dim by 0.164 mag ($\sim 14\%$) between 1890 and 1990 (Schaefer 2016), and lost $\sim 3\%$ of brightness during the 4.25yrs of *Kepler* mission (Montet & Simon 2016). The century-long dimming has been challenged by Hippke et al. (2016) and Lund et al. (2016). The distance estimates from *Gaia*’s DR1 parallax ($391.4^{+122.1}_{-75.2}$ pc, Hippke & Angerhausen (2016)) cannot constrain the absolute magnitude of the star. To resolve the controversy whether this star has dimmed considerably over 130 years (and perhaps more so earlier), it is crucial to gather more data.

2. METHOD

The plate photometry used in the previous long-term studies was taken by the Harvard College Observatory, which observed large portions of the sky repeatedly between 1886 and 1992. The photographs were taken on glass plates mainly with a blue-sensitive emulsion. The plates were digitized with a high speed scanner (Simcoe et al. 2006). The initial photometry and astrometry are described in Laycock et al. (2010) and Servillat et al. (2011), and the current progress is summarized in Tang et al. (2013). Today, the archive can be accessed over the Internet (DASCH, Digital Access to a Sky Century @ Harvard) (Grindlay et al. 2009; Laycock et al. 2010; Grindlay & Griffin 2012; Grindlay et al. 2012).

A major issue for long-term photometry spanning 130 years were changes in emulsion, filters, geographic locations, aging of optics, and the use of 16 different telescopes (Hippke et al. 2016). These changes might introduce small offsets in zeropoints, on the level of < 0.1 mag, and are very hard to determine and remove from time series. Also, observations ceased in the 1960s during the so-called “Menzel gap”, when organizational changes reduced the observatory activities. It has been speculated that Boyajian’s Star has undergone a dimming event in this decade (Montet & Simon 2016). Data

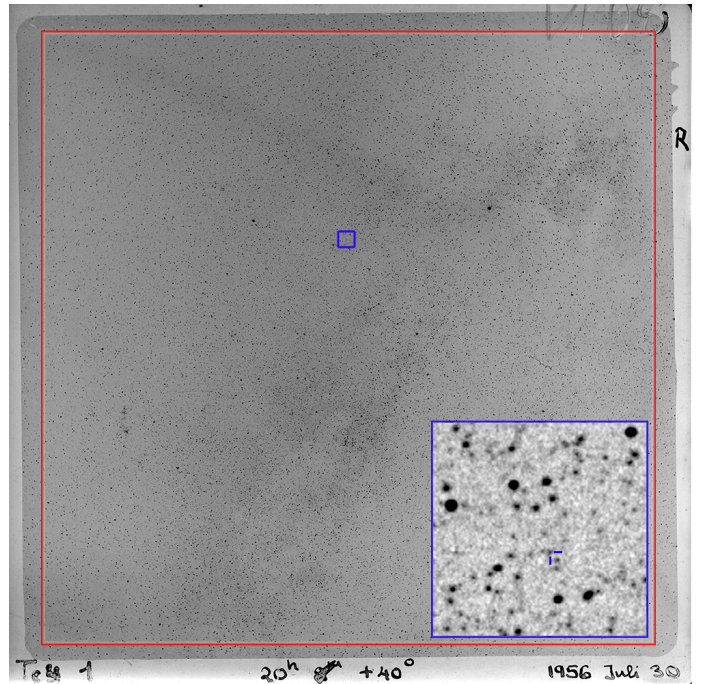


Figure 1. A Sonneberg Sky Patrol plate of average, representative quality taken on 30-July 1956. Cropped to the inner 90% of the image (red line) to remove annotations, and some of the vignetting and lens distortion towards the borders. The blue frame inset shows the region around Boyajian’s Star (cross-hairs).

from other sources could shed more light on the star’s brightness behavior.

2.1. Sonneberg Plate Archive

The second largest plate archive in the world, after Harvard, is located at Sonneberg Observatory (Bräuer & Fuhrmann 1992). The archive was fed by two different observation programs: the Sky Patrol, taken with 14 short-focus cameras of the same optics, plate sizes and emulsions, covered the entire sky between about 1935 and 2010 in a very homogeneous manner in two color bands, *pg* (blue) and *pv* (red) (Bräuer & Fuhrmann 1992; Bräuer et al. 1999). The deeper Field Patrol aimed at recording about 80 selected areas mostly along the Milky Way and the Galactic North Pole. The archive contains a total of about 275,000 plates.

For this study we have used the Sky Patrol plates of 13×13 cm² size, a scale of 830 arc sec per mm, giving a field size of about $26^\circ \times 26^\circ$. The limiting magnitudes are of the order of 14.5 mag in *pg* and 13.5 mag in *pv*, but the average limit achieved is about one mag brighter than these values. Plate scanning was initially performed with a digitalization machine, but subsequently upgraded with more, and more modern, scanners. Scan resolution was 15 μ m at 16 bit data depth.

Sonneberg plates have been used in previous studies, including novae (Collazzi et al. 2009; Goranskij et al.

2010; Johnson et al. 2014), protostellar stars (Xiao et al. 2010), RR Lyrae (Haussler et al. 2010), RS CVn binaries (Fröhlich et al. 2006) and other variables (Vogt et al. 2004; Vogt & Kroll 2005).

2.2. Sonneberg photometry Pipeline

The studies mentioned in the previous section often used visual estimates to derive the magnitudes. Common tools were loupes, microscopes and iris diaphragm photometers. Some studies used custom-made digital extraction pipelines. All methods performed very similarly, with typical scatter of order 0.15 mag for individual measurements. A systematic digital analysis by Vogt et al. (2004) (their section 3) yields scatter of 0.07...0.12 mag depending on stellar brightness and location on the plate. This study is also very interesting as it asks “How many ‘constant’ stars are in fact long-term variables?”, and presents many figures, each comparing a constant reference star to a newly found variable, sometimes with decade-long periods. About 85% of randomly selected stars are found to be constant within their uncertainty of 0.1 mag per century.

In order to maximize robustness, we used an established pipeline to reduce the images, closely resembling the process of the APPLAUSE project in the digitization of the plate archives in Hamburg, Bamberg and Potsdam (Tuvikene et al. 2014). The plate negatives are first inverted and then cropped to the inner 90% area of the scanned images, in order to exclude the glass borders and annotations. Then, we perform an astrometric solution with the Astrometry.net software (Lang et al. 2010) using a list of coordinates of the brightest sources as an input and the Tycho-2 catalog as a reference. For our wide-field images of $26^\circ \times 26^\circ$ we have a resolution of 17.5 arc seconds per scanned pixel, and the astrometric solution yields a global fit with errors of several pixels, due to lens distortions. Therefore, we split the image into mosaics of $\sim 7 \times 7^\circ$ and re-run the astrometry software for each mosaic individually. Afterwards, the astrometric errors are much smaller (few arc sec) than the pixel scale. Therefore, we do not further improve the astrometric solution through cross-calibration, which could be done by software packages like SCAMP (Bertin 2006). Of course, pairs of stars with separations smaller than the pixel scale get blended. Our object of interest, Boyajian’s Star, is fortunately located so that its neighbor stars of similar brightness are always separated by several pixels (Figure 1), even in bad seeing and overexposed plates. Boyajian’s Star is almost always located within the inner $\sim 30\%$ from the center of the plate. Due to some overlap in the Sonneberg Sky Patrol, there are further plates in the archive which are nominally taken at a different sky position, but have the star still on glass, mostly towards the corners or edges, and thus the star’s imprint will suffer from astigmatism. An extensive search for such plates could be done in case of further interest, but is beyond the scope of this paper.

After obtaining star coordinates, we perform photometry using the SExtractor program (Bertin & Arnouts 1996) which identifies all sources above a specified brightness threshold. SExtractor works on scans of photographic plates as well as CCDs. In principle, the program could be calibrated with the specific response curve of the scanner used to digitize the plates, and to specific photographic emulsions. However, it has been shown that it is preferred not to do this, as each plate has slight individual differences. Instead, it is recommended to use the default configuration of SExtractor (“standard mode”). This results in a non-linear magnitude scale, which has to be corrected using a number of constant calibration stars in post-processing (e.g., Kolesnikova et al. 2008; Wertz et al. 2016, and references therein). We tried both methods, and got virtually identical results for stars of the same brightness, as expected. SExtractor offers several aperture settings, and we got the smallest scatter when using a constant circular aperture.

Then, we follow the procedure described in Tang et al. (2013) for the photometric calibration of the DASCH plates. Each plate is divided in sub-fields, and a series of nearby comparison stars (using catalog values) is used to calibrate each star. This is similar to what people do when examining the plates by eye: The target object is compared with neighboring stars of similar magnitudes. Due to subtle changes over time, e.g. in emulsions, color sensitivity may change. This may introduce trends of a few tenths of a magnitude. It is crucial to have comparison stars as close in color to the program star as possible. By adding comparison stars of different colors one gets a synthetic comparison star with a mean color index of the stars. If the mean color index differs from the color index of the program star, then there will still be magnitude shifts with variations in the emulsion.

Therefore, we cannot blindly re-use the 8 comparison stars in Montet & Simon (2016) and the 2 stars from Schaefer (2016). Instead, we use the Tycho-2 catalog and select stars within 0.5 mag in brightness from our program star, within 1 degree distance, and within 0.1 mag of color difference in Tycho-2 $BT - VT$. This gives a total of 39 comparison stars.

In each epoch, we create one artificial “reference star” from the mean magnitudes of these comparison stars. As we selected stars very similar in brightness and color, the overall mean difference between the program star and the reference star is very small, 0.01 mag in brightness. With this method, we obtain a differential magnitude for our program star for each epoch. As we are not interested in standard magnitudes, we did not tie the mean magnitudes to a catalogue value. In the future, one might determine the color response of Sonneberg pg and pv and shift the magnitudes slightly for these colors. We estimate the differences between pg and BT , and between pv and BV , to be < 0.1 mag.

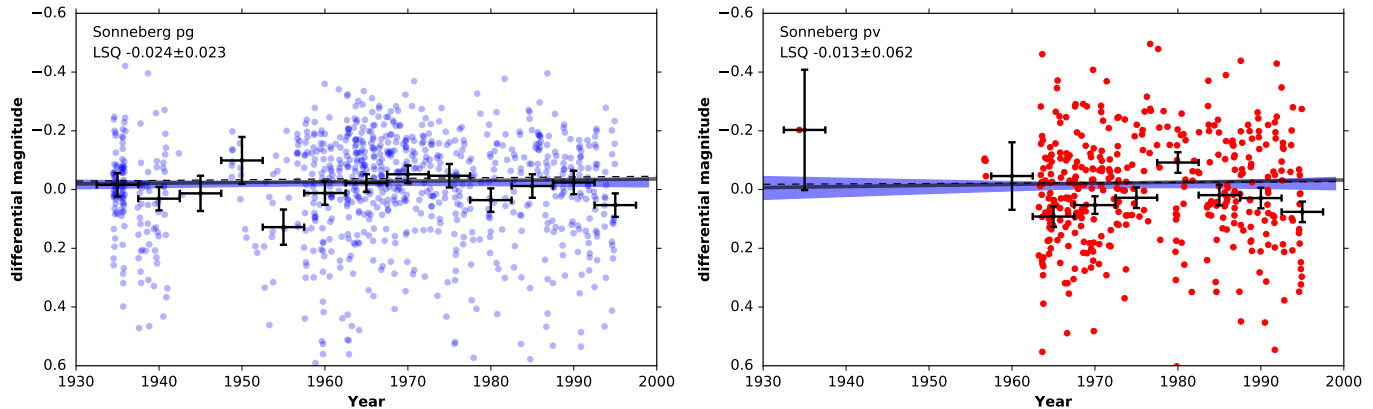


Figure 2. Sonneberg photometry for Boyajian’s Star in *pg* (blue) and *pv* (red) as differential magnitudes with respect to an artificial reference star. Each plot shows a linear least-squares regression (dashed line), a robust regression using the maximum likelihood method (solid gray line), and a linear MCMC regression with 1σ uncertainties (blue area). The regressions were made using the individual data points including their uncertainties as estimated by SExtractor; the 5-year bins are only shown for visibility.

The SExtractor solution of a single plate contains on average 120,000 identified sources, and usable photometry for 100,000 stars. After the calibration, the average standard deviation of Boyajian’s Star, compared to its mean magnitude, is 0.18 mag per plate in *pg* and 0.2 mag in *pv*. These values are comparable to other studies using Sonneberg plates (section 2.1), and photographic plates in general; e.g., Schaefer (2010). The described procedure produces 1263 magnitudes from a total of 1645 plates. As a quality filter, we remove all magnitudes of Boyajian’s Star where its calculated astrometric position is located outside of the star image, which is usually $\sim 2 - 3$ pixels. This removes 13 measurements, and eliminates the risk to mix up identifications. The remainder of 369 plates were rejected by SExtractor. Visual examination of 20 of the rejected plates showed that glass/emulsion defects and failure of star tracking were the most common issues. We have not attempted to recover these plates. We also decided against further quality cuts, such as measurements near the plate limit, and instead use all values including their (larger) uncertainties.

After inspection of the light curves, we identified a few prominent outliers. Several were around the year 1977, on plates Te15-5219, Te15-5148 and Te15-5611 (ScanIDs 411469, 411461 and 411488). Visual inspection of the plates showed prominent dirt on the glass. We have removed these data points.

For reproducibility and independent re-analysis, we make the relevant raw photometry open source¹.

3. RESULTS

¹ Due to the enormous data volume, please contact Peter Kroll (pk@4pisysteme.de) to agree on a transfer method.

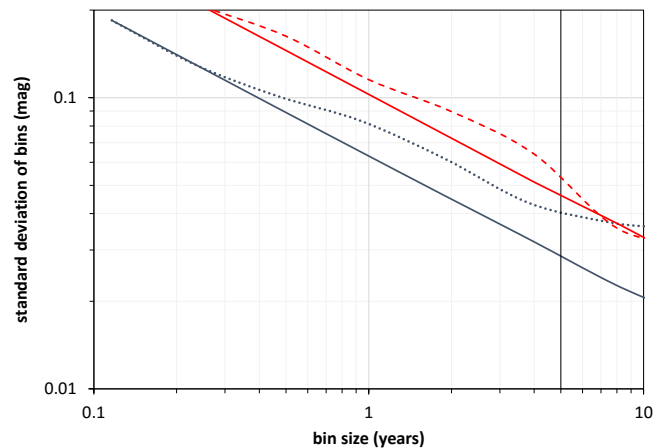


Figure 3. Comparison of the bin-ability for *pv* (red dashed) and theoretical pure white Gaussian noise (straight red); the same for *pg* in blue. The 5-year bins are marked with a vertical line. Typical real achieved uncertainties for 5-year bins of *pv* data are 0.05 mag, for *pg* it is 0.04 mag.

In the following sections, we discuss photometry from Sonneberg as well as other sources. Most magnitudes are reported in *B*, however these have different zeropoints due to the different use of filters and photographic emulsions. Unless otherwise noted, we have not modified the magnitudes, but left them as reported in the given sources. That is, we do not focus on absolute brightness comparisons, but on relative changes for each set of observations individually.

3.1. Lightcurve with Sonneberg data

We show the Sonneberg data for Boyajian’s Star in Figure 2. To search for trends, we performed a least-squares linear regression (with, and without the indi-

vidual uncertainties of the data points as measured by SExtractor). We ran regression separately for each passband, and also merged as one dataset.

We tested the photometry for normality and found strong statistical evidence for a non-Gaussian distribution. To account for this, we also performed a robust regression using the maximum likelihood method including the individual uncertainties of the data points, usually around 0.18 mag per plate in *pg* and 0.2 mag in *pv* as reported by SExtractor. Finally, we performed a linear Markov chain Monte Carlo (MCMC) regression using the *emcee* toolkit (Foreman-Mackey et al. 2013) and estimate the uncertainties. Results from all methods are consistent within their errors. All methods yield slope parameters consistent with zero. All results are shown in Table 1. We release the data and code to reproduce the results as open source².

This result is consistent with no dimming of the star between 1934 and 1995.

We checked the 39 comparison stars and found that several exhibit traces of variability, but these effects cancel out in the “masterflat” due to the large number of comparison stars. We show examples of comparison stars in the appendix (Figure 7). A more extensive study, yielding light curves for 100,000 stars from these plates, is planned for the future, but outside of the scope of this paper.

3.1.1. Check for seasonal variations

Due to the location of the Sonneberg observatory (50° 22′ 38.5″N, 11° 11′ 23.3″E), observation conditions are more favorable in the second half of the year. Indeed, the majority of plates (83%) were taken between the months of June and November. During this time, the local climate changes from warmer summer temperatures (> 25°C) to colder winter temperatures (< -5°C), while humidity is higher in autumn and lower in the summer and winter seasons. We checked the magnitudes for a possible correlation with the observation month, perhaps caused by changes in temperature, humidity, or air mass. We sorted the months by their average temperatures, and performed regressions versus the magnitudes. Also, we made monthly bins and compared their mean magnitudes to the overall mean. No significant correlation was found in either passband in any test. We conclude that the data do not show any obvious seasonal trend or variation.

3.1.2. Check for other meta-data

Meta-data for the Sonneberg photometry is available and contains the date and time of each plate, integration time, the camera which was used, and some limited information on the emulsion specification. We checked for correlations of magnitudes and camera, as well as for

emulsion specification. No correlation was found. One might imagine further tests, including the estimated air-mass during the integration time, which may effect color response; but such models are beyond the scope of this paper.

3.1.3. Trends on shorter timescales

To check the data for trends on shorter timescales, we performed a local polynomial smoothing using a Gaussian kernel function with a 5-year half-width (Figure 4, top and middle panel). In parallel, we binned the data in 5-year bins for comparison with Schaefer (2016).

Due to the non-Gaussian errors, the uncertainties of bins do not scale with \sqrt{N} . In order to derive credible uncertainties for the 5-year bins, we re-binned the data 1000 times with a moving boxcar, and calculated the average standard deviation of the bins in each run ex post. In other words, we test-binned the data many times in different segments, and measured the achieved gain from binning. The resulting uncertainties are 30-50% higher than using the simple \sqrt{N} calculation, and are adopted as minimum uncertainties in Figure 4. Typically, we find uncertainties of 0.05 mag in 5-year bins of *pv* data, and 0.04 mag for *pg* (compare Figure 3). We show these larger uncertainties for the 5-year bins in Figure 4, and leave the local polynomial smoothing with Gaussian uncertainties. This way, we can visually see the relevant impact of the effect: The achieved uncertainties after binning are larger than would be expected from Gaussian scatter. The shaded areas, representing Gaussian errors, are under-estimated.

For *pg*, we find a marginally significant ($\sim 2\sigma$) brightening around 1970 in the smoothed polynomial. At this time, DASCH and *pv* show nominal flux. This could be interpreted either as noise in the *pg* data, or, if astrophysical, as a blue-shift color-change (Figure 4, bottom panel). As the polynomial underestimates the uncertainties, it is more likely to be noise.

The DASCH data suggests that the main dimming, if real, occurred between 1955 and 1965. This is not seen in *pg* (and *pv* has insufficient data for this time).

For the time between 1980 and 1995, we find a dimming trend in both colors (marginally significant at $\sim 2\sigma$). However, as a similar brightening is seen in *pg* for earlier times, which is not reflected in DASCH data, this is most likely due to remaining systematics in the data.

During other times, deviations from nominal flux are minor and can not be considered significant within our limits of ~ 0.05 mag ($\sim 5\%$) per 5-year bin/half-width.

3.1.4. Literature comparison

We can test the hypothesis of a trend of 0.164 mag per century as suggested in Schaefer (2016) using a t-test (or F-test) for the β -parameter (slope) of the regression. The result indicates that a slope of 0.164 mag per century is in disagreement with the data by 4.9σ

² <https://www.github.com/hippke/sonneberg>

Table 1. Regression results for the Sonneberg data

Method	Dataset	n	Slope (mag per century)
LSQ without uncertainties	pg	861	-0.007 ± 0.037
LSQ with uncertainties	pg	861	-0.024 ± 0.023
Maximum likelihood with uncertainties	pg	861	-0.024 (n/a)
MCMC with uncertainties	pg	861	$-0.009^{+0.008}_{-0.009}$
LSQ without uncertainties	pv	397	-0.002 ± 0.087
LSQ with uncertainties	pv	397	-0.013 ± 0.062
Maximum likelihood with uncertainties	pv	397	-0.037 (n/a)
MCMC with uncertainties	pv	397	$-0.014^{+0.010}_{-0.019}$
LSQ without uncertainties	pg + pv	1258	-0.006 ± 0.032
LSQ with uncertainties	pg + pv	1258	-0.009 ± 0.020
Maximum likelihood with uncertainties	pg + pv	1258	-0.017 (n/a)
MCMC with uncertainties	pg + pv	1258	$-0.005^{+0.004}_{-0.007}$

($F = 25.07, p < 0.0001$). This applies to *pg*, to *pv*, and to the combined data. The discrepancy with the claimed dimming is visually obvious as shown in Figure 5.

3.2. Lightcurve with APPLAUSE data

The APPLAUSE project digitizes photographic plates in the archives of Hamburg, Bamberg and Potsdam observatories (Groote et al. 2014; Tuvikene et al. 2014). The plates are digitized with high-resolution flatbed scanners. As of August 2016, 42,789 plates have been scanned and reduced³. These data have been used e.g. in a study on the historic long-term variability of active galaxies (Wertz et al. 2016). We have extracted the magnitudes for Boyajian’s Star using the public web interface. A first analysis showed a correlation of the star’s brightness with its position on the plate, which will be corrected in the next data release. For Boyajian’s Star, this accounts for 0.15 mag extra scatter. We have reduced the scatter by subtracting the mean magnitude of the annular bin (there are 8 annular bins). For a least-squares linear regression, this is irrelevant, as it does not change the slope of the fit. The result is a dimming of 0.61 ± 0.21 mag/century, inconsistent with all other data from Harvard, Sonneberg and Pulkovo (Figure 6, middle).

The slope in the APPLAUSE light curve is strongly affected by the data points from 1938–1939. These data originate from a telescope at the Hamburg Observatory that has strong coma effect in the images. The other data points come from three other telescopes. The APPLAUSE data is heterogeneous, with various telescopes and a wide range of emulsions and exposure times used,

so calibration is an issue. Also, photometry has been calibrated globally, without choosing local comparison stars for Boyajian’s Star. Such calibrations might be performed in a future data release. At the moment, however, the APPLAUSE data suffers from large systematics in the case of Boyajian’s Star and cannot be used for an individual analysis.

3.3. Lightcurve with Pulkovo data

Pulkovo observatory is the main astronomical observatory of the Russian Academy of Sciences, located outside of St. Petersburg. It was founded in 1839 and the regular photographic observations were started at in 1894. The collection today contains 50,000 plates (Kanaev et al. 2002). The plates were measured using the “Ascorecord” machine with visual pointing, the “Fantasy” automatic complex (Gerasimov et al. 1989), and the UMAX scanner (600 ppi) (Izmailov et al. 2016). In 2010, the measurement and calibration technique for wide fields digitized by the scanner Microtec (3200 ppi) was developed. About 2000 plates with asteroids observations were digitized and measured (Khrutskaya et al. 2011). These data were used for e.g. studies on Pluto (Khrutskaya et al. 2013). The plates were taken with the “Normal Astrograph”, with 330 mm aperture and 3467 mm focal length, between 1922 and 2001. The plates’ emulsion had a maximum sensitivity close to the B-band (440–450 nm). For Boyajian’s Star, we decided to use a digital camera for plate digitization. The plate digitization and calibration process is described in (Izmailov et al. 2016) and used 9 nearby stars for calibration. The average standard deviation from the mean is 0.13 mag. A least-squares regression yields 0.07 ± 0.22 mag/century (Figure 6, bottom). Due to the low number of data points, any one point already changes the result signifi-

³ <http://dx.doi.org/10.17876/plate/dr.2/>, accessed 26-August 2016.

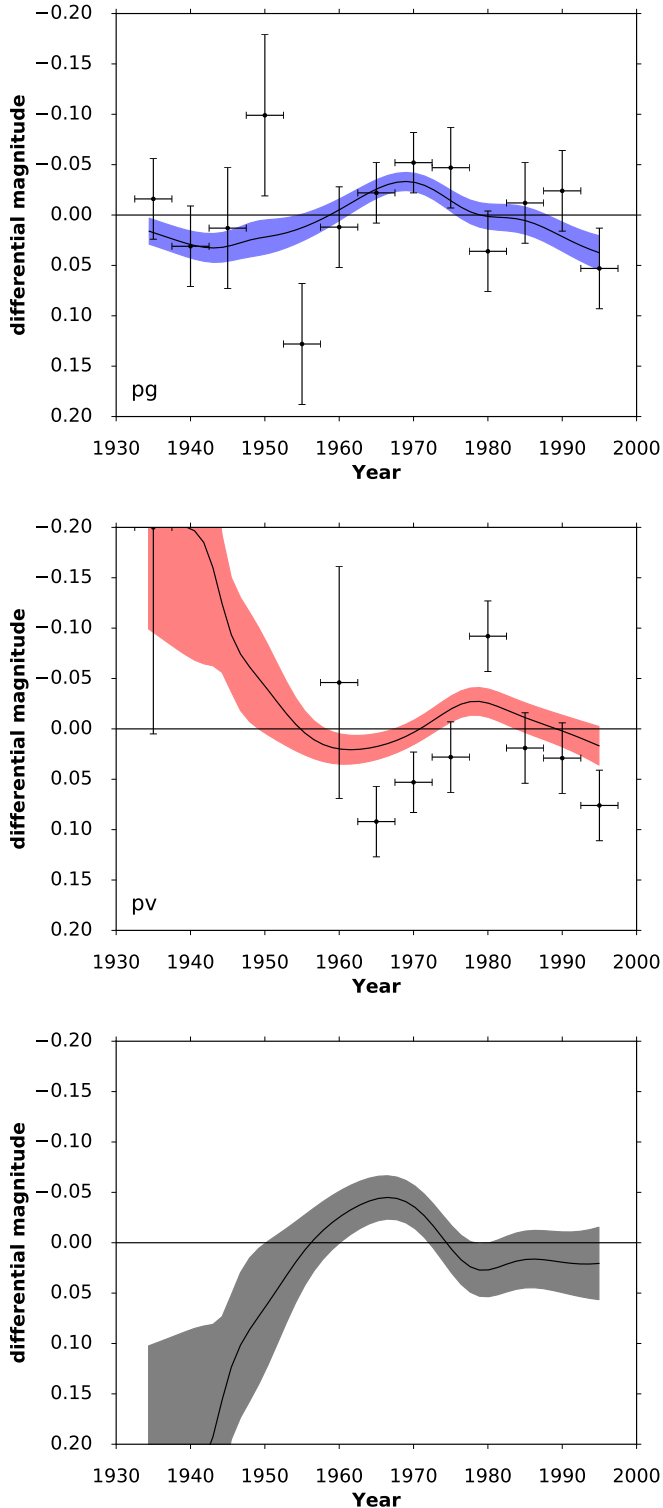


Figure 4. Top, middle: Local polynomial smoothing using a Gaussian kernel function with a 5-year half-width (solid line) with 1σ uncertainties (shaded areas). The analysis was performed on the individual data points, but for visibility we show the 5-year bins only. Bottom: $pg - pv$ giving the color difference (redder color in positive values). Note that no pv data is available for the 1940s; the trend shown at this time is fitted by the algorithm but can not be used for interpretation.

cantly. Therefore, the Pulkovo data cannot be used for an individual analysis of Boyajian’s Star.

3.4. Lightcurve with DASCH data

These data were discussed extensively in Hippke et al. (2016). For comparison, we show all APASS-calibrated data without quality cuts, resulting in a slope of 0.12 mag instead of 0.16 mag per century as suggested by Schaefer (2016) (Figure 6, top).

3.5. Period search

Boyajian et al. (2016) discuss several periodic signals (their section 2.1). The rotation period of the star is found to be 0.88 d (Boyajian et al. 2016), although this period has been claimed to originate from a different star (Makarov & Goldin 2016). From the separation of dips, a possible period of a circumstellar body is identified, at 48.4 or 48.8 d (or half this value). Finally, the largest dips are separated by 726 d. In order to search for such periodicities in our historic data, we combined all photometry (DASCH, Sonneberg, AP-PLAUSE, Pulkovo), and normalized the flux values per observatory by their median. Each measurement (plate) received the same weight.

For sinusoidal trends, such as the rotation signal, the Lomb-Scargle (LS) periodogram is most sensitive. It is the generalized form of the Fourier transforms and handles gaps in the data without introducing spurious power (Scargle 1982; Horne & Baliunas 1986; Zechmeister & Kürster 2009). For transit-like events, the Box-fitting Least Squares (BLS) algorithm (Kovács et al. 2002) is more suitable. It fits the input time series to periodic “box”-shaped functions, rather than decomposing it into sinusoids. The BLS has been run for periods up to 50 years, and transit durations between 1 hour and 10 days.

Both methods, LS and BLS, we find only peaks that are yearly aliases, and a few caused by single outliers. When these are ignored, no significant peaks remain. We tested the sensitivity to a 48.8 d transit signal through injection and retrieval. We find that a 10% dip of 1-day length, repeating regularly every 48.8 d, would have been detected with $> 3\sigma$ confidence. Consequently, we can constraint transits to $< 10\%$ in depth for periods < 50 d. For 726-day signals, we cannot give useful limits due to insufficient data caused by many gaps.

4. DISCUSSION

If we take the results of constant flux (within the limits of $\sim 5\%$ per 5-year bin) at face value, it is still possible that the star undergoes periodic changes in brightness. A brightness variation of $\sim 3\%$ over a few years, as reported by Montet & Simon (2016), is compatible with the Sonneberg (and DASCH) data, and invisible in their noise.

Lacki (2016) recently discussed possible time spans for a potential dimming phenomenon. For example, if the star would have dimmed continuously as it likely did

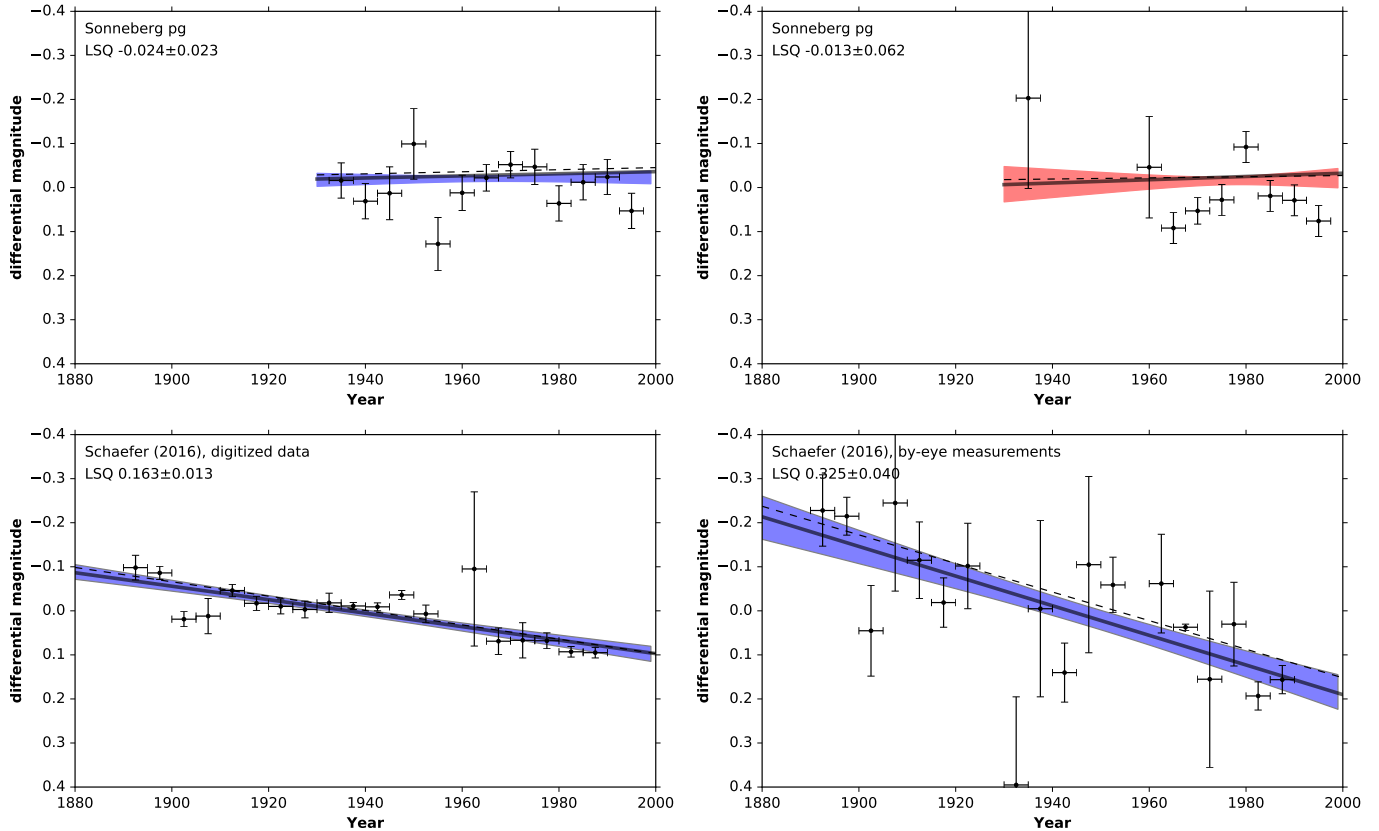


Figure 5. Comparison of Sonneberg and DASCH data using the same axes scales. Each plot shows the data in 5-year bins, a linear least-squares regression (dashed line), a robust regression using the maximum likelihood method (solid gray line), and a linear MCMC regression with 1σ uncertainties (shaded areas). The Sonneberg panels have been regressed with the individual data points; the 5-year bins are only shown for comparison. The data in the bottom panels are taken from Table 2 in [Schaefer \(2016\)](#).

during the Kepler mission time, it would have been a million times brighter ($V=2.45$) in ancient times (2,500 years ago), and it should appear in star catalogs of this time (which we checked, and which is not the case). Also, such a brightness variation is in strong tension with the star being of type F3V in a distance of $391.4^{+53.6}_{-42.0}$ pc ([Hippke & Angerhausen 2016](#)). With the Gaia distance estimate, and the known luminosity of an F3V star, we can constraint the brightness to be nominal within $\sim 20\%$.

Consequently, the duration of brightness changes might be larger than a few years, but shorter than 2,500 years (and shorter than ~ 150 years, if the Gaia result is not affected from systematics). Perhaps the star exhibits periodic decade-long fluctuations at a level of a few percent.

5. CONCLUSION

We have analyzed photometry from the Sonneberg observatory, and other sources, and found strong evidence that Boyajian’s Star has not dimmed, but kept a constant flux between 1934 and 1995. Variations on 5-year scale are found to be of order 5% or less. We found no evidence for any periodicity, neither sinusoidal, nor transit-like.

T.T. acknowledges support by the Estonian Ministry of Education and Research (IUT26-2, IUT40-2) and by the European Regional Development Fund (TK133).

APPENDIX

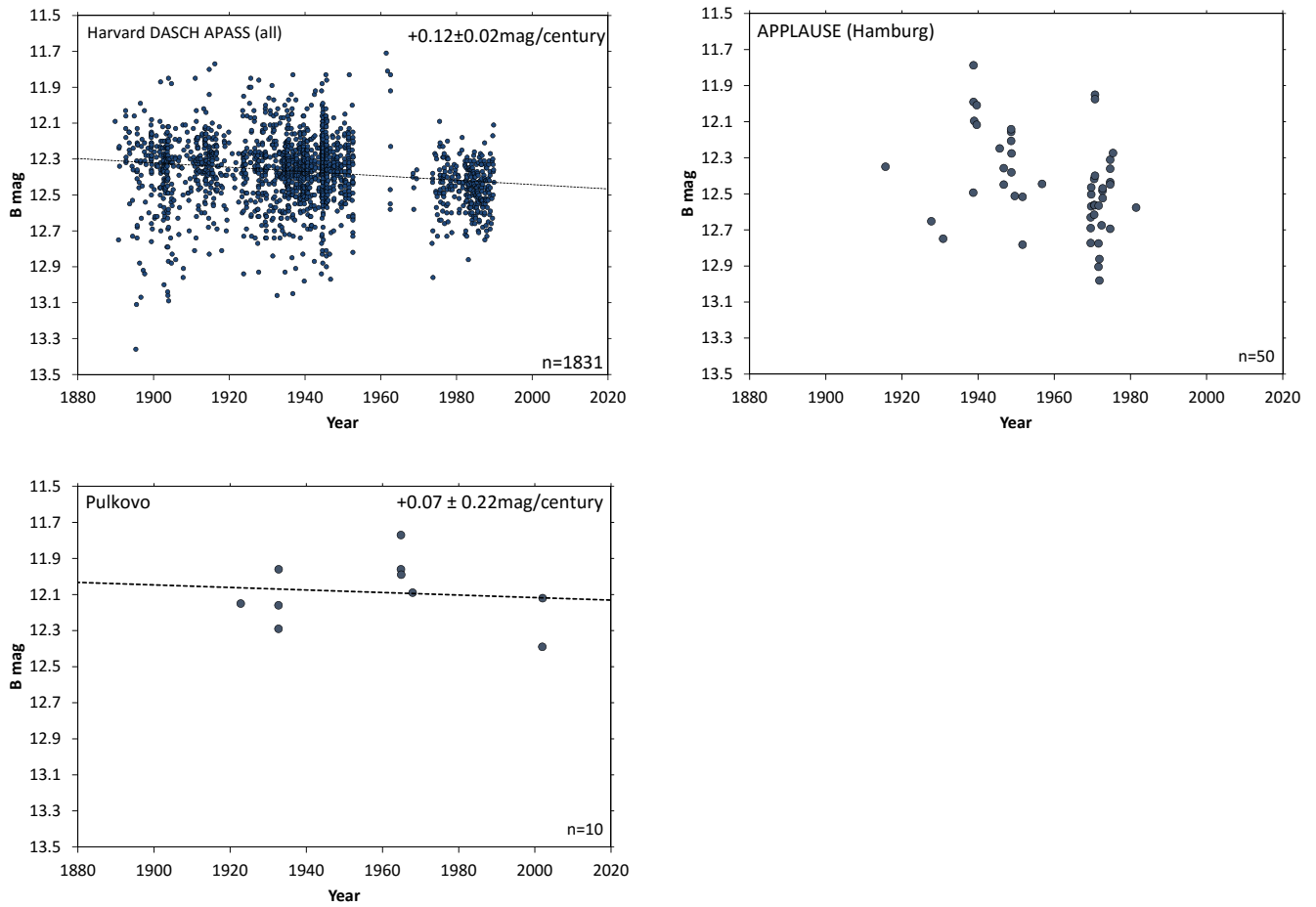


Figure 6. Photometry from DASCH (top left), APPLAUSE (top right) and Pulkovo (bottom left).

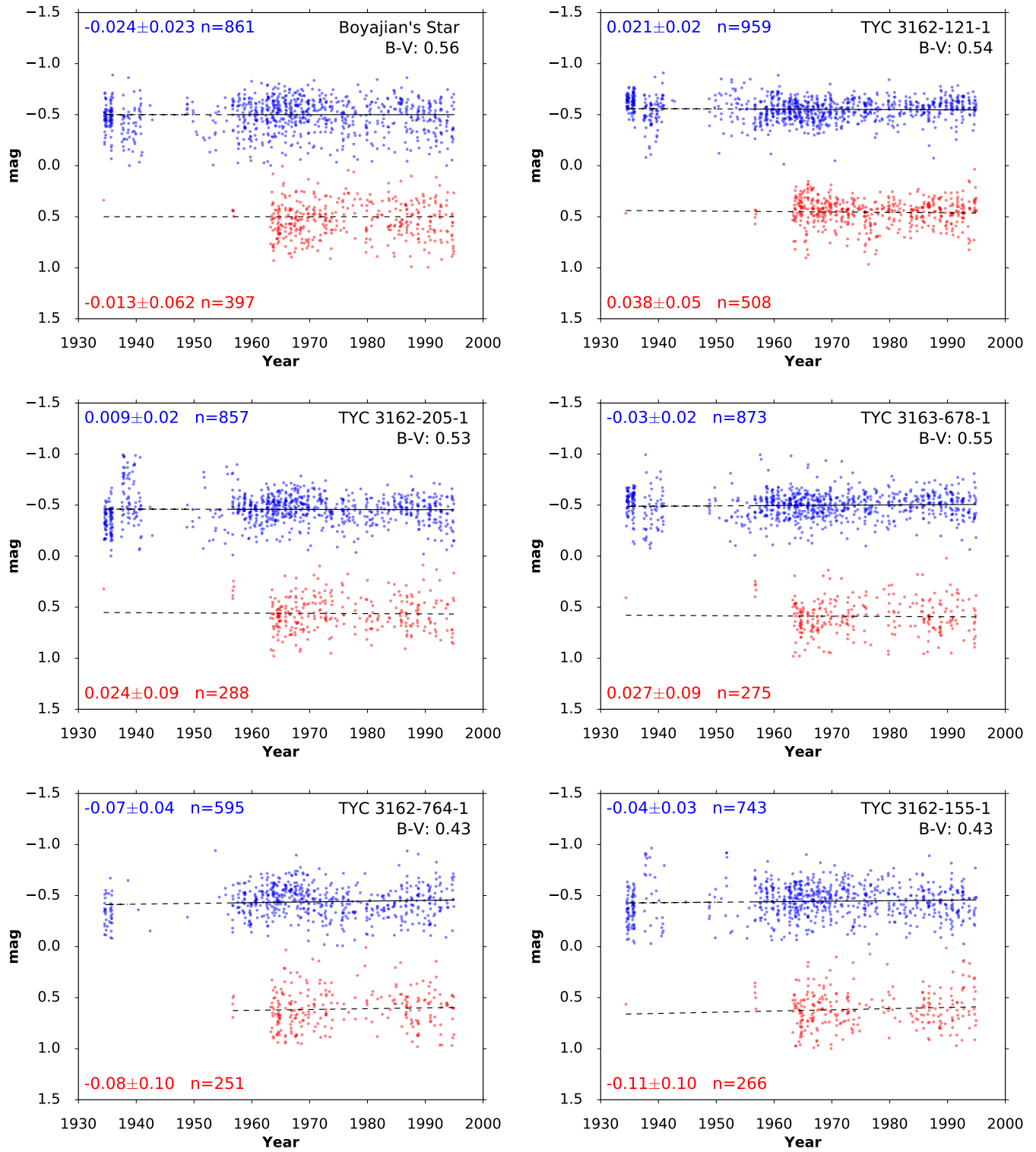


Figure 7. Examples of comparison stars. The program star, Boyajian's Star, is shown on the upper left for comparison. Differential magnitudes have been offset to -0.5 for *pg* and +0.5 for *pv* for better visibility.

REFERENCES

- Abeyssekara, A. U., Archambault, S., Archer, A., et al. 2016, *ApJL*, 818, L33
- Bertin, E. 2006, in *Astronomical Society of the Pacific Conference Series*, Vol. 351, *Astronomical Data Analysis Software and Systems XV*, ed. C. Gabriel, C. Arviset, D. Ponz, & S. Enrique, 112
- Bertin, E., & Arnouts, S. 1996, *A&AS*, 117, 393
- Bodman, E. H. L., & Quillen, A. 2016, *ApJL*, 819, L34
- Borucki, W. J., Koch, D., Basri, G., et al. 2010, *Science*, 327, 977
- Boyajian, T. S., LaCourse, D. M., Rappaport, S. A., et al. 2016, *MNRAS*, 457, 3988
- Bräuer, H.-J., & Fuhrmann, B. 1992, *Die Sterne*, 68, 19
- Bräuer, H.-J., Häusele, I., Löchel, K., & Polko, N. 1999, *Acta Historica Astronomiae*, 6, 70
- Collazzi, A. C., Schaefer, B. E., Xiao, L., et al. 2009, *AJ*, 138, 1846
- Foreman-Mackey, D., Hogg, D. W., Lang, D., & Goodman, J. 2013, *PASP*, 125, 306
- Fröhlich, H.-E., Kroll, P., & Strassmeier, K. G. 2006, *A&A*, 454, 295
- Gerasimov, A. G., Polyakov, V. B., Polyakov, E. V., Sokolov, A. V., & Tsekmejster, S. D. 1989, *Wissenschaftliche Zeitschrift*, 38, 28
- Goranskij, V., Shugarov, S., Zharova, A., Kroll, P., & Barsukova, E. A. 2010, *Peremennye Zvezdy*, 30, arXiv:1011.6063
- Grindlay, J., Tang, S., Los, E., & Servillat, M. 2012, in *IAU Symposium*, Vol. 285, *New Horizons in Time Domain Astronomy*, ed. E. Griffin, R. Hanisch, & R. Seaman, 29–34
- Grindlay, J., Tang, S., Simcoe, R., et al. 2009, in *Astronomical Society of the Pacific Conference Series*, Vol. 410, *Preserving Astronomy's Photographic Legacy: Current State and the Future of North American Astronomical Plates*, ed. W. Osborn & L. Robbins, 101
- Grindlay, J. E., & Griffin, R. E. 2012, in *IAU Symposium*, Vol. 285, *New Horizons in Time Domain Astronomy*, ed. E. Griffin, R. Hanisch, & R. Seaman, 243–248
- Groote, D., Tuvikene, T., Edelmann, H., et al. 2014, in *Astroplate 2014*, 53
- Harp, G. R., Richards, J., Shostak, S., et al. 2016, *ApJ*, 825, 155
- Hausser, K., Berthold, T., & Kroll, P. 2010, *Information Bulletin on Variable Stars*, 5926
- Hippke, M., & Angerhausen, D. 2016, *ArXiv e-prints*, arXiv:1609.05492
- Hippke, M., Angerhausen, D., Lund, M. B., Pepper, J., & Stassun, K. G. 2016, *ApJ*, 825, 73
- Hippke, M., Learned, J. G., Zee, A., et al. 2015, *ApJ*, 798, 42
- Horne, J. H., & Baliunas, S. L. 1986, *ApJ*, 302, 757
- Huber, D., Bedding, T. R., Stello, D., et al. 2011, *ApJ*, 743, 143
- Izmailov, I. S., Roshchina, E. A., Kiselev, A. A., et al. 2016, *Astronomy Letters*, 42, 41
- Johnson, C. B., Schaefer, B. E., Kroll, P., & Henden, A. A. 2014, *ApJL*, 780, L25
- Kanaev, I., Kanaeva, N., Poliakov, E., & Pugatch, T. 2002, in *Russian Information, Computing and Telecommunication Resources for Supporting Basic Research*
- Khrutskaya, E. V., De Cuyper, J.-P., Kalinin, S. I., Berezhnoy, A. A., & de Decker, G. 2013, *ArXiv e-prints*, arXiv:1310.7502
- Khrutskaya, E. V., Khovritchev, M. Y., Berezhnoy, A. A., Kalinin, S. I., & Shakht, N. A. 2011, in *Gaia follow-up network for the solar system objects: Gaia FUN-SSO workshop proceedings, held at IMCCE -Paris Observatory, France, November 29 - December 1, 2010 / edited by Paolo Tanga, William Thuillot.* - ISBN 2-910015-63-7, p. 131-135, ed. P. Tanga & W. Thuillot, 131–135
- Kolesnikova, D. M., Sat, L. A., Sokolovsky, K. V., Antipin, S. V., & Samus, N. N. 2008, *AcA*, 58, 279
- Kovács, G., Zucker, S., & Mazeh, T. 2002, *A&A*, 391, 369
- Lacki, B. C. 2016, *ArXiv e-prints*, arXiv:1610.03219
- Lang, D., Hogg, D. W., Mierle, K., Blanton, M., & Roweis, S. 2010, *AJ*, 139, 1782
- Laycock, S., Tang, S., Grindlay, J., et al. 2010, *AJ*, 140, 1062
- Lisse, C. M., Sitko, M. L., & Marengo, M. 2015, *ApJL*, 815, L27
- Lund, M. B., Pepper, J., Stassun, K. G., Hippke, M., & Angerhausen, D. 2016, *ArXiv e-prints*, arXiv:1605.02760
- Makarov, V. V., & Goldin, A. 2016, *ArXiv e-prints*, arXiv:1609.04032
- Marengo, M., Hulsebus, A., & Willis, S. 2015, *ApJL*, 814, L15
- Montet, B. T., & Simon, J. D. 2016, *ApJL*, 830, L39
- Scargle, J. D. 1982, *ApJ*, 263, 835
- Schaefer, B. E. 2010, *ApJS*, 187, 275
- . 2016, *ApJL*, 822, L34
- Schuetz, M., Vakoch, D. A., Shostak, S., & Richards, J. 2016, *ApJL*, 825, L5

- Servillat, M., Los, E. J., Grindlay, J. E., Tang, S., & Laycock, S. 2011, in *Astronomical Society of the Pacific Conference Series*, Vol. 442, *Astronomical Data Analysis Software and Systems XX*, ed. I. N. Evans, A. Accomazzi, D. J. Mink, & A. H. Rots, 273
- Simcoe, R. J., Grindlay, J. E., Los, E. J., et al. 2006, in *Proc. SPIE*, Vol. 6312, *Society of Photo-Optical Instrumentation Engineers (SPIE) Conference Series*, 631217
- Tang, S., Grindlay, J., Los, E., & Servillat, M. 2013, *PASP*, 125, 857
- Thompson, M. A., Scicluna, P., Kemper, F., et al. 2016, *MNRAS*, 458, L39
- Tuvikene, T., Edelmann, H., Groote, D., & Enke, H. 2014, in *Astroplate 2014*, 127
- Vogt, N., & Kroll, P. 2005, in *Astronomical Society of the Pacific Conference Series*, Vol. 335, *The Light-Time Effect in Astrophysics: Causes and cures of the O-C diagram*, ed. C. Sterken, 119
- Vogt, N., Kroll, P., & Splittgerber, E. 2004, *A&A*, 428, 925
- Wertz, M., Horns, D., Groote, D., et al. 2016, *ArXiv e-prints*, arXiv:1607.00312
- Wright, J. T., Cartier, K. M. S., Zhao, M., Jontof-Hutter, D., & Ford, E. B. 2016, *ApJ*, 816, 17
- Xiao, L., Kroll, P., & Henden, A. A. 2010, *AJ*, 139, 1527
- Zechmeister, M., & Kürster, M. 2009, *A&A*, 496, 577